IOP Publishing Physica Scripta
Phys. Scr. 95 (2020) 055805 (9pp) https://doi.org/10.1088/1402-4896/ab783f

Dynamic magnetic hysteresis loop behaviors of a mixed spin (2, 5/2) Ising model on two interpenetrating square lattices

Mustafa Keskin and Mehmet Ertaş[1]

Department of Physics, Erciyes University, 38039 Kayseri, Turkey

E-mail: keskin@erciyes.edu.tr and mehmetertas@erciyes.edu.tr

Received 25 October 2019, revised 31 January 2020
Accepted for publication 19 February 2020
Published 2 March 2020

Abstract

We investigate dynamic magnetic hysteresis loop (DMHL) behaviors of a mixed spin (2, 5/2) Ising model on two interpenetrating square lattices under an oscillating magnetic field within the effective-field theory based on Glauber–type stochastic dynamics. We study the DMHL properties for various values of reduced temperatures (T/zJ), crystal-field interaction (D/zJ) and frequency (w) of the magnetic field. We also examine T/zJ, D/zJ and w dependences of the coercive fields (CFs) and remanent magnetizations (RMs). We found that for very low and high values of T/zJ and D/zJ, the hysteresis loop area is narrower and thinner that correspond soft magnets that desirable for transformers and motor cores and AC applications. We observed that for high values of w, the hysteresis loop areas are wide and big that corresponds hard magnets which can be useful for permanent magnets, magnetic recording, small motors and magnetic locks. We also found that the DMHLs, CFs and RMs behaviors are in quantitatively good agreement with some theoretical for Ising systems and experimental works for magnetic materials, such as cobalt films, Fe films and some magnetic nanomaterials.

Keywords: mixed spin (2, 5/2) ising system, dynamic magnetic hysteresis, coercivity field, remanent magnetization, effective-field theory, glauber–type stochastic dynamics

(Some figures may appear in colour only in the online journal)

1. Introduction

In the preceding published paper [1], referred to as paper I, we have investigated the dynamic magnetic properties of a mixed spin (2, 5/2) Ising model on two interpenetrating square lattices under an oscillating (sinusoidal) magnetic field within the effective-field theory based on the Glauber–type stochastic dynamics that has been often called the dynamic effective-field theory (DEFT). First, we found the phases in the system by examining the time dependence of the magnetizations for various interaction parameter values. Then, we studied the thermal behavior of the dynamic magnetizations in which these investigations lead us to define the nature (a first- or second-order) of the dynamic phase transition (DPT) and to get the DPT points. Finally, the dynamic phase diagrams (DPDs) were constructed for various values of Hamiltonian parameters in the reduced temperature (T/zJ) and magnetic field amplitude (h_0/zJ) plane that display very rich and interesting dynamic critical phenomena, such as tricritical point, double critical end point, critical end point, zero-temperature critical point and triple point. Moreover, DPDs also contain paramagnetic, two different ferrimagnetic phases as well as several mixed phases.

On the other hand, the dynamic magnetic hysteresis loop (DMHL) behaviors are the one of the important subjects in the dynamic magnetic properties of the systems that were not investigated in paper I. Therefore, our aim in this paper is to examine the DMHL features of a mixed spin (2, 5/2) Ising system on two interpenetrating square lattices under an oscillating (sinusoidal) magnetic field within the DEFT. We study the DMHL behaviors for various values of reduced temperatures (T/zJ), crystal-field interaction (D/zJ) and

[1] Author to whom any correspondence should be addressed.

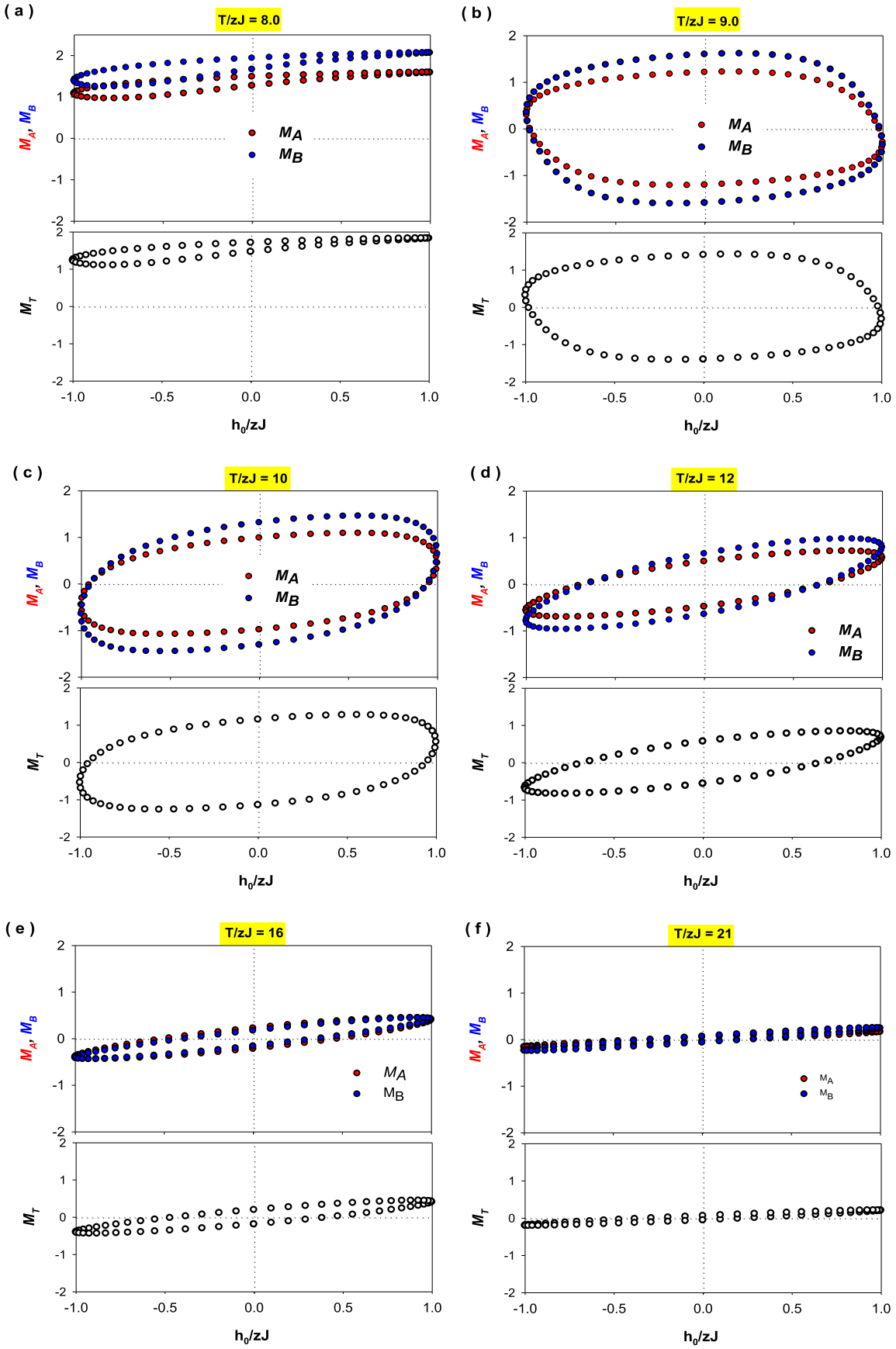

Figure 1. The DMHL behaviors various values of the reduced temperature dependence (T/zJ) for the magnetization of M_A, M_B, and M_T; $w = 0.05$ and D/zJ = 1.0.

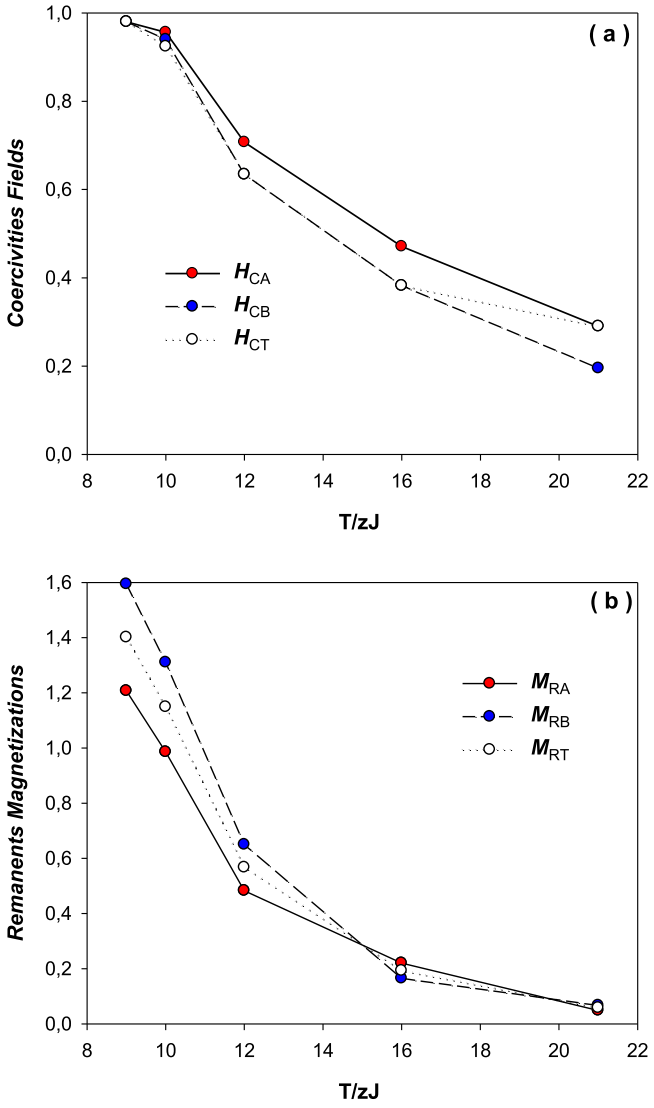

Figure 2. (a) The behavior of coercive fields and (b) the remanent magnetizations as the function of reduced temperature for the same parameter values as in figure 1.

frequency (w) of the magnetic field. We also investigate behaviors of the coercive fields and remanent magnetizations as a function of T/zJ, D/zJ and w.

We should also mention that the DMHL, often referred to as dynamics of magnetization reversal, has been the subject of intensive research for both experimental and theoretical researchers, due to its extensive advanced technological applications, namely high frequency devices, the developing memory storage devices, and also scientific research [2]. The DMHL is defined as the dependence of the hysteresis loop area on the frequency and the amplitude of the applied magnetic field [3]. The DMHL behaviors of various materials, namely thin [4] and ultrathin [5] Co films on a Cu (001) surface, epitaxial single ferromagnetic fcc NiFe (001), fcc Co(001) layers and NiFe/Cu/Co(001) spin-valve structures [6], Fe/GaAs(001) ultrathin films and epitaxial Fe/InAs (001) [7], ultrathin epitaxial Fe/GaAs (001) [8], permalloy thin films [9, 10], Fe and CoFe films [11], $[Co/Pt]_3$ magnetic multilayers [12], Fe thin films [13, 14], $Pb_{0.4}Sr_{0.6}TiO_3$ ferroelectrics film [15], single crystalline compound $Co_7(TeO_3)_4Br_6$, [16], the ternary intermetalic compound $DyMnSi_2$ [17] and BiGdFeCoO films [18], etc, have been studied. Moreover, the DMHL properties have been theoretically studied by mostly following three models [19]: (1) Ising kind models, namely spin-1/2, higher spin systems, namely spin-1, spin-3/2, spin-2 systems and mixed spin Ising models. (ii) Extended domain wall models. (iii) The time-dependent Landau–Lifshitz-Gilbert equations. The DMHL has been also investigate some other models, such as, the stochastic Landau–Lifshitz equation, semi-adiabatic theory, Neel-Brown theory, dynamic Preisach model, and Brown's model.

Also worth mentioning that the mixed spin (2, 5/2) Ising model is the most important as well as most used model among the mixed spin Ising systems. The reason is that it is the prototypical model to study the magnetic features of some molecular-based based magnetic materials, namely A $Fe^{II}Fe^{III}$ $(C_2O_4)_3$ [A = $N(n\text{-}C_nH_{2n+1})_4$ (see [20, 21] and references therein), $AM^{II}Fe^{III}$ $(C_2O_4)_3$ (A = $N(n\text{-}C_3H_7)$, M^{II} = Mn, Fe) [22, 23], $N(n\text{-}C_4H_9)_4$ $Fe^{II}Fe^{III}$ $(C_2O_4)_3$ (see [24, 25] and references therein). Moreover, the other advantages of the model that it also gives rich and interesting critical phenomena, such as rich and interesting phase diagrams, more critical points, multiple-cycle hysteresis behaviors, etc (see [1, 26, 27] and references therein).

2. Dynamic effective-field equations

A mixed spin (2, 5/2) Ising model consist of two interpenetrating square sublattices with spin-2 (states $\sigma = 0, \pm1, \pm2$) and with spin-5/2 (states $S = \pm1/2, \pm3/2$) on the sites of sublattices A and B, respectively. This mixed spin model has four order parameters, which have been introduced as follows: Two average magnetizations $\langle\sigma\rangle$ and $\langle S\rangle$ for the sublattices A and B, respectively that are the excess of one orientation over the other, frequently called the dipole moments. Two average quadrupole moments, $\langle q_A\rangle$, which is a linear function of average square magnetization, namely $\langle\sigma_i^2\text{-}2\rangle$, for the A sublattice and $\langle q_B\rangle$, which is a linear function of average square magnetization, $\langle S_j^2\text{-}35/12\rangle$, for the sublattice B. The Hamiltonian of this system is defined as

$$\mathcal{H} = -J\sum_{\langle ij\rangle}\sigma_i S_j - D\left(\sum_i \sigma_i^2 + \sum_j S_j^2\right) - h(t)\left(\sum_i \sigma_i + \sum_j S_j\right) \quad (1)$$

where $\langle ij\rangle$ is the interaction between the nearest neighbors spins on sites i and j. J represents the interactions between the particles with spin-2 and particles have spin-5/2; it has been called the nearest-neighbor bilinear exchange constant. The D is the essentially chemical potential, mostly called the single-ion anisotropy or crystal-field constant and $h(t)$ represents an

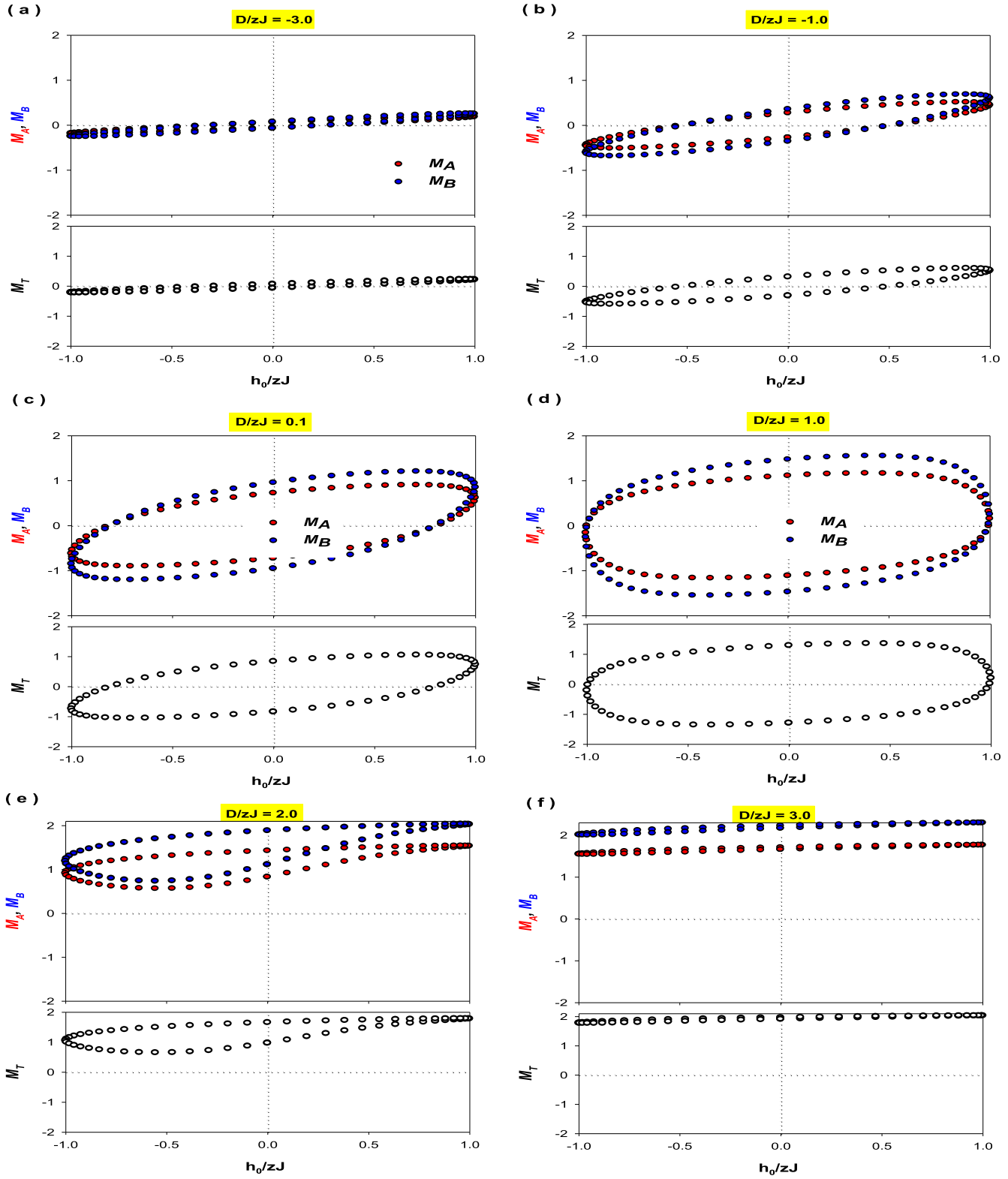

Figure 3. The DMHL behaviors various values of the reduced crystal-field interaction. (D/zJ) for the magnetization of M_A, M_B, and M_T; $w = 0.05\pi$, T/zJ = 9.5.

oscillating (sinusoidal) magnetic field and defined as

$$h_0(t) = h \sin(wt), \tag{2}$$

where $w = 2\pi\nu$ and h are, respectively, the angular frequency of the oscillating field and the amplitude. The system is in contact with an isothermal heat bath at absolute temperature. Since the derivative of the dynamic equations is extensively discussed in paper I, we will briefly give the derivative of these equations here. We have used the Glauber-type stochastic (GS) dynamics [28] to find the set of dynamic

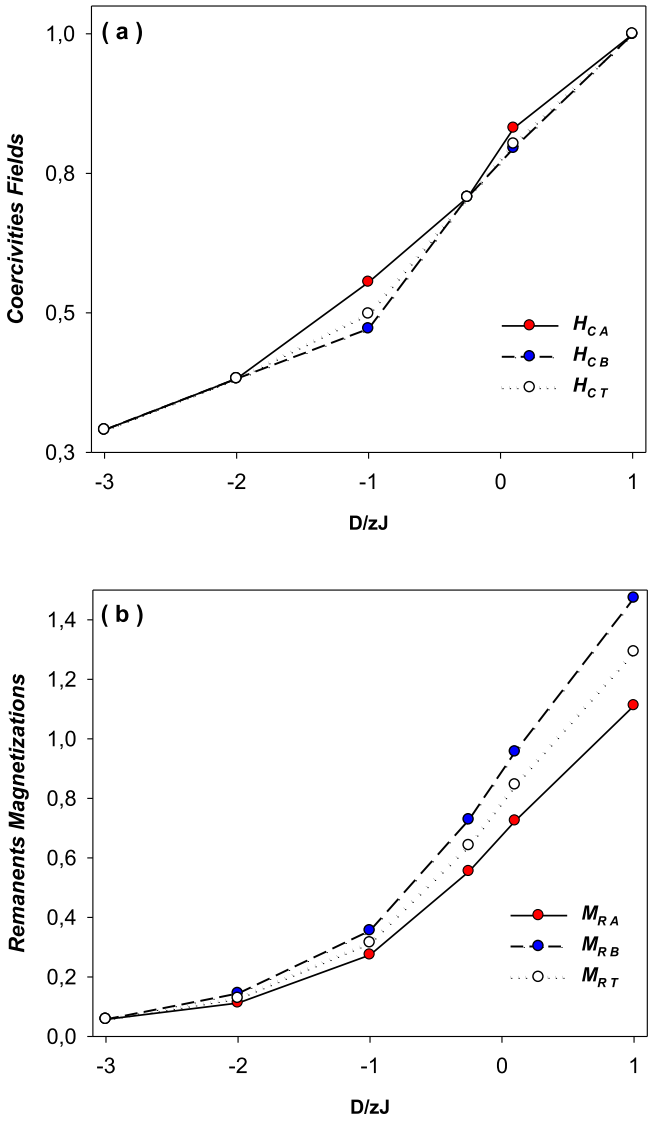

Figure 4. (a) The behavior of coercive fields and (b) the remanent magnetizations as the function of the D/zJ for the same parameter values as in figure 3.

$P^A(\sigma_1, \sigma_2,\ldots,\sigma_N;\ t)$ as the probability that the system has the σ-spin configuration $\sigma_1, \sigma_2,\ldots,\sigma_N;$ t, at time t while letting the S spins fixed for A sublattice. The similar probability, $P^B(S_1, S_2,\ldots,S_N;\ t)$, can also defined for the sublattice B. Then, we calculate $W_i^A(\sigma_i \to \sigma_i')$ and $W_j^B(S_j \to S_j')$, the probabilities per unit time that the ith σ spin changes from σ_i to σ_i' (while the S spins are momentarily fixed) and the j^{th} S spin changes from S_j to S_j' (while the σ spins are momentarily fixed), respectively. Thus, $P^A(\sigma_1, \sigma_2,\ldots,\sigma_N;\ t)$ can be written as

$$\begin{aligned}\frac{d}{dt}P^A(\sigma_1, \sigma_2,\ldots,\sigma_N;\ t)=&\\ -\sum_i\left(\sum_{\sigma_i\neq\sigma_i'}W_i^A(\sigma_i\to\sigma_i')\right)&\\ \times P^A(\sigma_1, \sigma_2,\ldots,\sigma_i,\ldots,\sigma_N;\ t)&\\ +\sum_i\left(\sum_{\sigma_i\neq\sigma_i'}W_i^A(\sigma_i'\to\sigma_i)\right)&\\ \times P^A(\sigma_1, \sigma_2,\ldots,\sigma_i',\ldots,\sigma_N;\ t),&\end{aligned} \tag{3}$$

where $W_i^A(\sigma_i \to \sigma_i')$ satisfies the detailed balance condition [1] and defined as

$$W_i^A(\sigma_i\to\sigma_i')=\frac{1}{\tau}\frac{\exp[-\beta\ \Delta E^A(\sigma_i\to\sigma_i')]}{\sum_{\sigma_i'}\exp[-\beta\ \Delta E^A(\sigma_i\to\sigma_i')]}, \tag{4}$$

where $\beta = 1/k_BT_A$, k_B is the Boltzmann factor, $\sigma_i' = \pm2, \pm1, 0$, and

$$\begin{aligned}\Delta E^A(\sigma_i\to\sigma_i')=-(\sigma_i-\sigma_i')\left(J\sum_j S_j^B+h(t)\right)&\\ -[(\sigma_i')^2-(\sigma_i)^2]D,&\end{aligned} \tag{5}$$

From the master equation associated with the stochastic process, it follows that the average $\langle\sigma_i^A\rangle$ satisfies the following equation:

$$\tau\frac{d}{dt}\langle\sigma_i^A\rangle=-\langle\sigma_i^A\rangle+\left\langle\frac{2\exp(4\beta D)\sin h(2\beta(E_i+h(t)))+\exp(\beta D)\sin h(\beta(E_i+h(t)))}{\exp(4\beta D)\cos h(2\beta(E_i+h(t)))+\exp(\beta D)\cos h(\beta(E_i+h(t)))+1/2}\right\rangle, \tag{6}$$

effective-field equations. The system evolves according to a GS process at a rate of $1/\tau$ transitions per unit time; hence, the frequency of spin flipping is $1/\tau$. We define where $\langle\ldots\rangle$ denotes the canonical thermal average and $E_i = J\sum_j S_j^B$. Performing the similar calculations, the dynamic equation for the sublattice B can be obtained as

$$\begin{aligned}\tau\frac{d}{dt}\langle S_j^B\rangle=&-\langle S_j^B\rangle\\ &+\left\langle\frac{5\sin h\left(\frac{5\beta}{2}(E_j+h(t))\right)+3\exp(-4\beta D)\sin h\left(\frac{3\beta}{2}(E_j+h(t))\right)+\exp(-6\beta D)\sin h\left(\frac{\beta}{2}(E_j+h(t))\right)}{2\cos h\left(\frac{5\beta}{2}(E_j+h(t))\right)+2\exp(-4\beta D)\cos h\left(\frac{3\beta}{2}(E_j+h(t))\right)+2\exp(-6\beta D)\cos h\left(\frac{\beta}{2}(E_j+h(t))\right)}\right\rangle,\end{aligned} \tag{7}$$

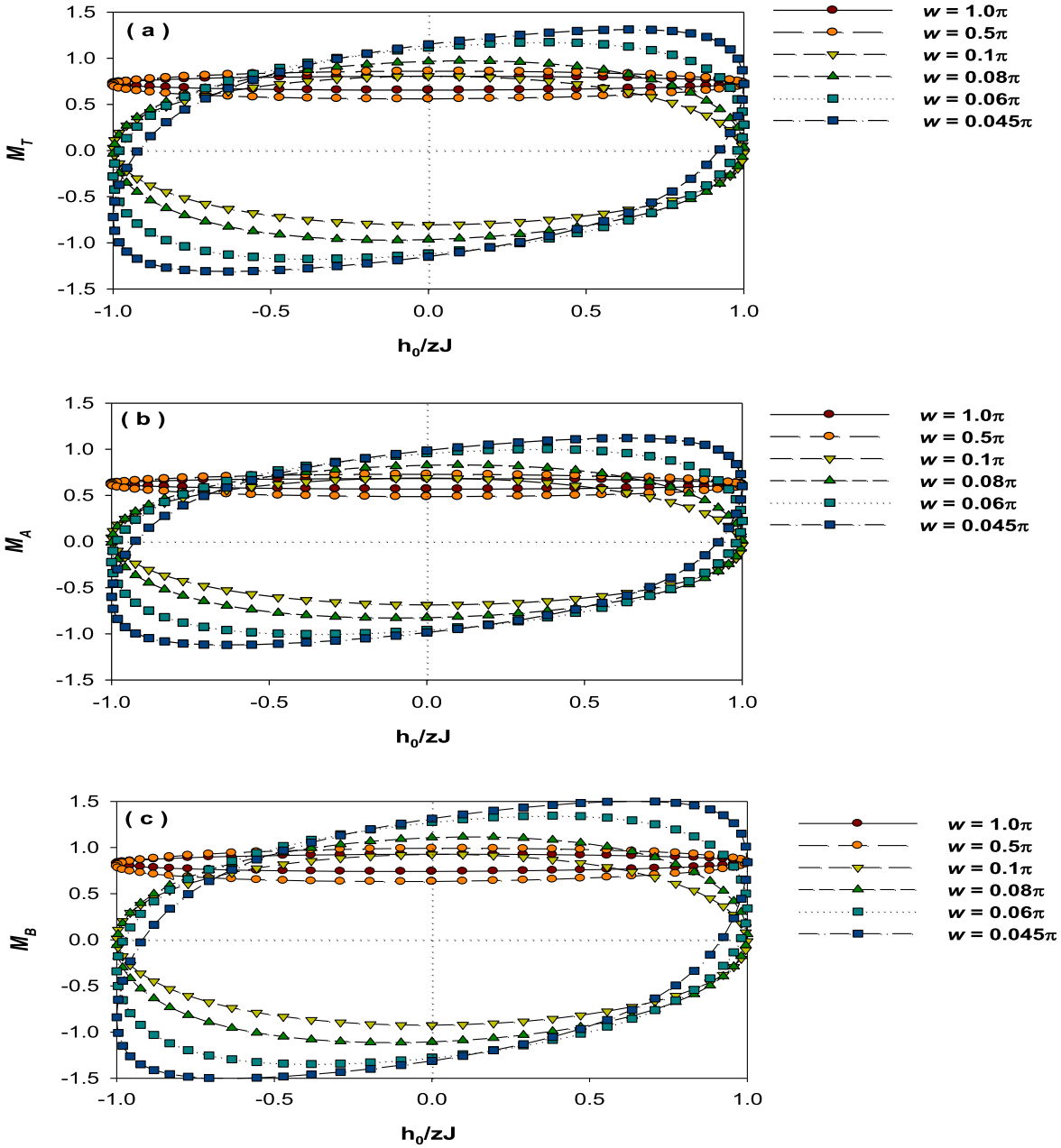

Figure 5. The oscillating field frequency (w) of DMHL behaviors for the magnetization of M_A, M_B, and M_T ; D/zJ = 1.0 and T/zJ = 10.

where $E_j = J\sum_i \sigma_i^A$.

In order to obtain the set of dynamic the effective-field theory (EFT) equations, we apply the EFT with correlations, introduced by Honmura and Kaneyoshi [29] and Kaneyoshi *et al* [30]. The main problem is to evaluate the thermal average of the last terms in equations (6) and (7). For this purpose, we have used the exact relation due to Callen [31] and the decoupling approximation that corresponds essentially to the Zernike approximation [32], thus the dynamic equations have been obtained for σ and S in paper I as

$$\begin{aligned}\frac{d}{dt}m_A = &-m_A + a_0 + a_1 m_B + a_2 {m_B}^2 \\ &+ a_3 {m_B}^3 + a_4 {m_B}^4 + a_5 {m_B}^5 + a_6 {m_B}^6 \\ &+ a_7 {m_B}^7 + a_8 {m_B}^8 + a_9 {m_B}^9 + a_{10} {m_B}^{10} \\ &+ a_{11} {m_B}^{11} + a_{12} {m_B}^{12} + a_{13} {m_B}^{13} + a_{14} {m_B}^{14} \\ &+ a_{15} {m_B}^{15} + a_{16} {m_B}^{16} + a_{17} {m_B}^{17} + a_{18} {m_B}^{18} \\ &+ a_{19} {m_B}^{19} + a_{20} {m_B}^{20}, \end{aligned} \quad (8)$$

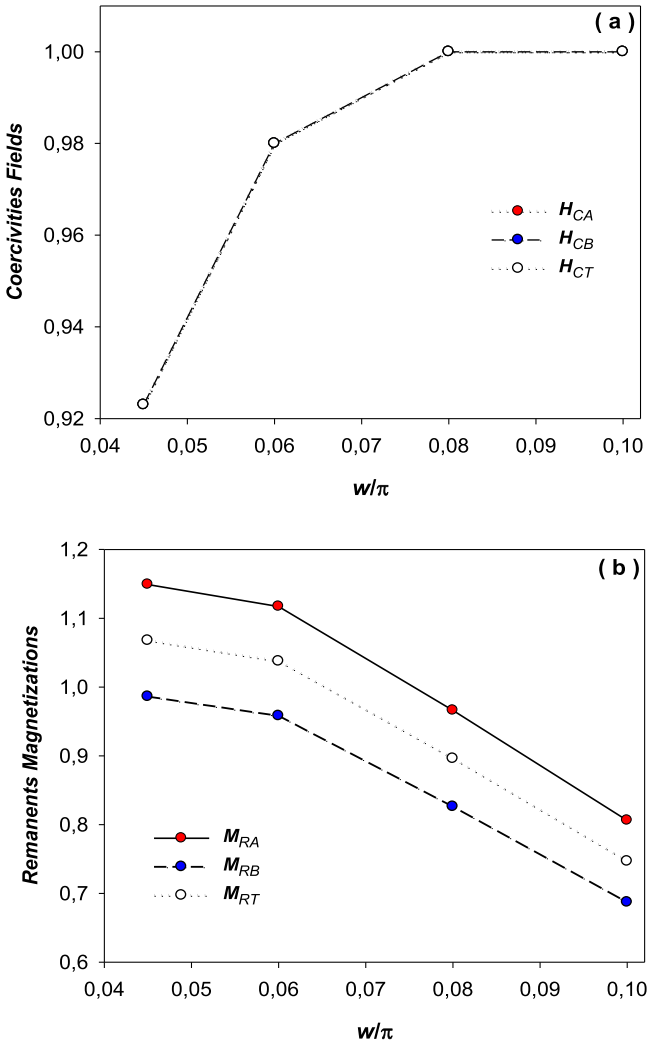

Figure 6. (a) The behavior of coercive fields and (b) the remanent magnetizations as the function of the w for the same parameter values as in figure 5.

and

$$\frac{d}{dt}m_B = -m_B + b_0 + b_1 m_A + b_2 {m_A}^2 + b_3 {m_A}^3 + b_4 {m_A}^4 + b_5 {m_A}^5 + b_6 {m_A}^6 + b_7 {m_A}^7 + b_8 {m_A}^8 + b_9 {m_A}^9 + b_{10} {m_A}^{10} + b_{11} {m_A}^{11} + b_{12} {m_A}^{12} + b_{13} {m_A}^{13} + b_{14} {m_A}^{14} + b_{15} {m_A}^{15} + b_{16} {m_A}^{16}. \quad (9)$$

The coefficients $a_i (i = 1, \ldots, 20)$ and $b_j (j = 1, \ldots, 16)$ are given in the appendix of paper I.

The dynamic magnetizations are defined as [3]

$$M_{A,B} = \frac{w}{2\pi} \oint m_{A,B}(t) dt. \quad (10)$$

Moreover, to investigate the DMHL properties one should define the hysteresis loop area [3], i.e.,

$$A = -\oint m_{A,B}(t) dh = -hw \oint m_{A,B}(t) \cos(wt) dt. \quad (11)$$

Numerical calculations of equation (11) give the DMHLs for the magnetizations of A and B sublattices. Total magnetization is described, as $M_T = (M_A + M_B)/2$ in which its numerical calculations provide the DMHL features of the total magnetization. We should also mention that numerical calculations are measured in unit zJ, where z is the number of nearest neighbor pair of spins; hence, the bilinear interaction (J) is restricted to the z. We should also mention that some researchers have been absorbed z in J. We numerically solve these equations and, results and discussions are given in section 3.

3. Results and discussion

Figure 1 illustrates DMHL behaviors various values of the reduced temperature dependence (T/zJ) for the magnetization of M_A, M_B, and M_T; $w = 0.05$ and D/zJ = 1.0. For low values of T/zJ, hysteresis curves display positive valued narrow loops then as the T/zJ increases, evolve into horizontal line with symmetrical ellipse like loops that they are increasing, then as the values of T/zJ increasing more, loop areas decreasing and finally becomes very small. Thus, this figure illustrates the type I behavior for small values T/zJ, then as the T/zJ increases it displays the type II behavior and the type III is seen at bigger values of T/zJ, according to classification of Punya *et al* [33] and Vatansever *et al* [34]. Similar DMHL behaviors have been also reported [35]. Experimentally, it is observed the similar DMHL properties in ultrathin Co films on a surface Cu(001) [4, 5], in [Co/Pt]3 magnetic multilayers [12] and in ultrathin epitaxial Fe films grown on a flat and stepped W(110) surface [13]. We should also mention that if the hysteresis loop area is big and wide that correspond hard magnets which can be useful for memory devices, magnetic recording and permanent magnets. On the other hand, if the hysteresis loop areas are narrower and thinner that correspond soft magnets in which desirable for transformers and motor cores and AC applications. Figures 2(a) and (b) display the reduced temperature dependence (T/zJ) of the coercive fields (CFs) and remanent magnetizations (RMs), respectively, with the same interaction parameters in figure 1. In figure 2, H_{CA}, H_{CB} and H_{CT} represent the CFs for magnetizations of sublattice A, sublattice B and the total magnetization, respectively. Moreover, M_{RA}, M_{RB} and M_{RT} are the RMs for the magnetizations of sublattices A, B and the total magnetization, respectively. Figure 2 shows that as the T/zJ increases the CFs and RMs decrease and very high values of T/zJ they become zero. Moreover, RMs are decreasing more rapidly than the CFs. Similar behaviors, quantitatively, have been observed the dynamic theoretical work [36] as well as with the theoretical works [37–39] and experimental reports [40–44] in the equilibrium cases.

Figure 3 displays DMHL behaviors different values of the reduced crystal-field dependence (D/zJ) for the M_A, M_B, and M_T; $w = 0.05\pi$, T/zJ = 9.5. For low values of D/zJ, hysteresis curves exhibit a symmetric, narrow and thinner ellipse like loops, as the D/zJ increases, the DMHL areas

growing; finally loop areas getting positive values of narrow and thinner loops and the symmetry is destroyed as increasing D/zJ. The similar behaviors have been theoretically observed [36,45–47]. Figures 4 (a) and (b) display the behaviors of CFs and RMs as a function of D/zJ, respectively, with the same parameters of figure 3. CFs and RMs increase as the D/zJ values increase. Moreover, CFs are increasing linearly, but RMs, exponentially. Similar features have also been seen in different Ising systems [48, 49].

Figure 5 shows the influence of w on the DMHL behaviors for the M_A, M_B, and M_T; D/zJ = 1.0 and T/zJ = 10. From the figure, we observe that the for high values of w, hysteresis curves display positive valued narrow loops and as the w values decrease, the loops evolve into horizontal line with ellipse like loops and their areas growing. Moreover, DMHLs develope the symmetric shape while w values increasing. The similar DMHLs have been reported theoretically in various Ising systems [35, 50, 51] and experimental reports [4, 5, 52]. Figures 6(a) and (b) illustrate the behaviors of CFs and RMs as a function of w, respectively, with the same parameters of figure 5. The CFs increase with increasing w values and finally become constant for higher values of w. On the other hand, RMs decrease while w increases finally become zero for larger values w and similar behaviors for figure 6(a) have been theoretically found [51, 52].

4. Conclusions

The DMHL behaviors of a mixed spin (2, 5/2) Ising model on two interpenetrating square lattices under a time-dependent (sinusoidal) magnetic field are studied within the DEFT. In particular, the DMHL properties for different values of reduced temperatures (T/zJ), crystal-field interaction (D/zJ) and frequency (w) of the magnetic field are investigated. We also examine T/zJ, D/zJ and w dependences of the CFs and RMs. We found that for very low and high values of T/zJ and D/zJ, the hysteresis loop areas are thinner and narrower that correspond soft magnets in which desirable for transformers and motor cores and AC applications. For small values of w, the hysteresis loop areas are wide and big that correspond hard magnets which can be useful for magnetic recording, memory devices and permanent magnets. Finally, we should point out that, as far as we know; DMHLs in molecular based magnetic materials have not been studied experimentally; hence, we could not compare our results with some experimental results of molecular-based magnetic materials. Moreover, some of obtained results are compared with available theoretical and experimental works and find a quantitatively good agreement with some theoretical [35–39, 45–51] and experimental works [4, 5, 12, 13, 40–44, 52].

ORCID iDs

Mustafa Keskin https://orcid.org/0000-0003-4700-3439

References

[1] Ertaş M, Deviren B and Keskin M 2012 *Phys. Rev. E* **86** 051110
[2] Chakrabarti K and Acharyya M 1999 *Rev. Mod. Phys.* **71** 847
[3] Bertotti G 1998 *Hysteresis in Magnetism* (San Diego: Academic)
[4] Suen J S, Lee M H, Teeter G and Eskine J L 1999 *Phys. Rev. B* **59** 4249
[5] Jiang Q, Yang H N and Wang G C 1995 *Phys. Rev. B* **52** 14911
[6] Lee W Y, Samed A, Moore T A, Bland J A C and Choi B C 2000 *J. Appl. Phys.* **87** 6600
[7] Moore T A, Rothman J, Xu Y B and Bland J A C 2001 *J. Appl. Phys.* **89** 7018
[8] Moore T A, Wastlbauer G, Blanda J A C, Cambril E, Natali M, Decanini D and Chen Y 2003 *J. Appl. Phys.* **93** 8746
[9] Nistor C, Faraggi E and Erskine J L 2005 *Phys. Rev. B* **72** 014404
[10] Moore T A, Hayward T J, Tse D H Y, Bland J A C, Castano F J and Ross C A 2005 *J. Appl. Phys.* **97** 063910
[11] Steinke N J, Moore T A, Mansell R, Bland J A C and Barnes C H W 2012 *Rev. B* **86** 184434
[12] Robb D T, Xu Y H, Hellwig O, McCord J, Berger A, Novotny M A and Rikvold P A 2008 *Phys. Rev. B* **78** 134422
[13] Suen J S and Eskine J L 1997 *Phys. Rev. Lett.* **18** 3567
[14] Cao Y, Xu K, Jiang W, Droubay T, Ramuhalli P, Edwards D, Johnson B R and McCloy J 2015 *J. Magn. Magn. Mater.* **395** 361
[15] Li K, Li T, Du D, Remiens D, Dong X and Wang G 2014 *Solid State Commun.* **192** 89
[16] Prester M, Zivkovic I, Drobac D, Surija V, Pajic D and Berger H 2011 *Phys. Rev. B* **84** 064441
[17] dos Reis D C, Franca E L T, De Paula V G, Dos Santos A O, Coelho A A, Cardoso L P and Da Silva L M 2017 *J. Magn. Magn. Mater.* **424** 84
[18] Kuang D, Tang P, Yang S and Zhang Y 2016 *J. Magn. Magn. Mater.* **397** 33
[19] Keskin M and Ertaş M 2017 *J. Supercond. Nov. Magn.* **30** 3439
[20] Li J, Du A and Wei G 2004 *Physica B* **348** 79
[21] Wei G, Zhang Q, Xin Z and Liang Y 2004 *J. Magn. Magn. Mater.* **277** 1
[22] Wei G, Zhang Q, Zhao J and Gy Y 2004 *Physica B* **381** 6
[23] Nakamura Y 2000 *J. Phys. Condens. Matter* **12** 4067
[24] Jiang W, Wang W, Zhang F and Ren W J 2009 *J. Appl. Phys.* **105** 07E321
[25] Yüksel Y 2013 *Phys. Lett. A* **377** 2494
[26] Wu H J, Wei) W, Wang F, Li B C, Li Q and Xu J H 2020 *J. Phys. Chem. Solids* **136** 109174
[27] Espriella N D L, Mercado C A and Buendia G M 2016 *J. Magn. Magn. Mater.* **417** 30
[28] Glauber R J 1963 *J. Math. Phys.* **4** 294
[29] Honmura R and Kaneyoshi T 1979 *J. Phys. C: Solid State Phys.* **12** 3979
[30] Kaneyoshi T, Fittipaldi I P, Honmura R and Manabe T 1981 *Phys. Rev. B* **24** 481
[31] Callen H B 1963 *Phys. Lett.* **4** 161
[32] Zernike F 1940 *Physica* **7** 565
[33] Punya A, Yimnirum R, Laoratanakul P and Laosiritaworn Y 2010 *Physica B* **405** 3482
[34] Vatansever E, Akıncı Ü, Yüksel Y and Polat H 2013 *J. Magn. Magn. Mater.* **329** 14
[35] Aktaş B O, Akıncı Ü and Polat H 2014 *Phys. Rev. E* **90** 012129
[36] Kantar E and Ertaş M 2015 *J. Supercond. Nov. Magn.* **28** 2529
[37] Şarlı N and Keskin M 2012 *Solid State Commun.* **152** 354
[38] Kantar E 2016 *J. Alloy. Compd.* **76** 337
[39] Kamalakar G, Hwang D W and Hwang L P 2002 *J. Mater. Chem.* **12** 1819

[40] Sort J, Dieny B, Fraune M, Koenig C, Lunnebach F, Beschoten B and Güntherodt G 2004 *Appl. Phys. Lett.* **84** 3696
[41] Curiale J, Sanchez R D, Troiani H E, Leyva A G and Levy P 2005 *Appl. Phys. Lett.* **87** 043113
[42] Zang L and Zang Y 2009 *J. Magn. Magn. Mater.* **321** L15
[43] Fleaca C T, Morjan I, Alexandrescu R, Dumitrache F, Soare I, Gavrila-Florescu L, Le Normand F and Derory A 2009 *Appl. Sur. Sci.* **255** 5386
[44] Garcia J A, Bertran E, Elbaile L, Garcia-Cespedes J and Svalov A 2010 *Phys. Stat. Sol. C* **7** 2679
[45] Vatansever E and Polat H 2015 *Thin Solid Films* **589** 778
[46] Ertaş M, Keskin M and Deviren B 2012 *J. Stat. Phys.* **146** 1244
[47] Cerruti B and Zapperi S 2007 *Phys. Rev. B* **75** 064416
[48] Cerruti B, Durin D and Zapperi S 2008 *Physica B* **403** 422
[49] Hu R, Soh A K, Zheng G P and Ni Y 2006 *J. Magn. Magn. Mater.* **301** 458
[50] Wang L, Teng B H, Rong Y H, Lu Y and Wang Z C 2012 *Solid State Commun.* **152** 1641
[51] Yüksel Y, Akıncı Ü and Polat H 2013 *Phys. Status Solidi b* **250** 196
[52] Jiang Q, Yang H-N and Wang G C 1996 *J. Appl. Phys.* **79** 5122